NH_2-terminal fragments of the 130 kDa subunit of myosin phosphatase increase the Ca^{2+} sensitivity of porcine renal artery

Yinbi Zhou, Katsuya Hirano, Chie Sakihara, Junji Nishimura and Hideo Kanaide

Division of Molecular Cardiology, Research Institute of Angiocardiology, Faculty of Medicine, Kyushu University, Fukuoka 812-8582, Japan

(Received 8 October 1998; accepted after revision 5 January 1999)

1. The effects of the NH_2-terminal fragments of M130, a 130 kDa regulatory subunit of smooth muscle myosin phosphatase, on contraction and myosin light chain phosphorylation were investigated in Triton X-100-permeabilized porcine renal artery.

2. Incubation of the permeabilized fibres with $M130^{1\text{-}633}$ (a fragment containing amino acid residues 1–633) or $M130^{44\text{-}633}$ enhanced the Ca^{2+}-induced contraction and shifted the $[Ca^{2+}]_i$–force relationship to the left (EC_{50} of Ca^{2+}: 330 nM, control, without fragment; 145 nM, $M130^{1\text{-}633}$; 163 nM, $M130^{44\text{-}633}$). Pre-incubation for 1–3 h was needed for these long constructs.

3. $M130^{1\text{-}374}$, $M130^{304\text{-}511}$ and $M130^{297\text{-}374}$, i.e. relatively short constructs compared with $M130^{1\text{-}633}$ and $M130^{44\text{-}633}$, also induced leftward shifts of the $[Ca^{2+}]_i$–force relationship (EC_{50} of Ca^{2+}: 65 nM, 72 nM and 180 nM, respectively). However, these required no pre-incubation.

4. Deletion of residues 304–374 from the most potent construct, $M130^{1\text{-}374}$, abolished the Ca^{2+}-sensitizing effect.

5. Wortmannin inhibited the enhancement of contraction induced by M130 fragments when added before contraction was initiated and partially inhibited the effects when added after steady-state contraction.

6. $M130^{1\text{-}374}$ slowed the rate of relaxation in Ca^{2+}-free medium. The time for 50% relaxation with this fragment was 510 ± 51 s, compared with 274 ± 14 s for control.

7. The levels of myosin light chain phosphorylation (22·4%) and force (34·5%) obtained with 300 nM Ca^{2+} were increased by 3 μM $M130^{1\text{-}374}$ to 35·7 and 92·2%, respectively. However, $M130^{1\text{-}374}$ had no effect on the phosphorylation–force relationship.

8. In conclusion, the NH_2-terminal M130 fragments containing residues 304–374 inhibited myosin phosphatase, increased myosin light chain phosphorylation and increased the Ca^{2+} sensitivity of the contractile apparatus in permeabilized porcine renal artery.

Reversible phosphorylation of the myosin light chains (MLCs) is one of the most important mechanisms for the regulation of smooth muscle contraction and relaxation (Hartshorne, 1987; Somlyo & Somlyo, 1994). The extent of MLC phosphorylation is regulated by the balance of two processes: phosphorylation and dephosphorylation catalysed by MLC kinase (MLCK) and MLC phosphatase (MLCP), respectively (Somlyo & Somlyo, 1994). Since the activity of MLCK is regulated by the Ca^{2+}–calmodulin complex, the cytosolic Ca^{2+} concentration ($[Ca^{2+}]_i$) has long been regarded as the major determinant of smooth muscle contraction, while the activity of MLCP was assumed to remain constant (Hartshorne, 1987). However, simultaneous measurement of $[Ca^{2+}]_i$ and force revealed that the relationship between $[Ca^{2+}]_i$ and force in smooth muscle varies with the type of stimulation inducing contraction or relaxation (Morgan & Morgan, 1984; Kanaide, 1995). This was also clearly demonstrated using permeabilized fibres, in which agonist and GTP-γ-S increased force at a constant $[Ca^{2+}]_i$ level (Nishimura *et al.* 1988). Thus, it is now widely accepted that alteration of the Ca^{2+} sensitivity of the contractile apparatus as well as changes in the Ca^{2+} level are important for the regulation of smooth muscle contraction (Somlyo & Somlyo, 1994). Concerning the mechanism for this change in Ca^{2+} sensitivity, it has been suggested that regulation of MLCP activity is one of the important mechanisms in the regulation of Ca^{2+} sensitivity (Somlyo *et al.* 1989). More recent experimental evidence suggests that inhibition of

MLCP activity is linked to an increase in Ca^{2+} sensitivity (Kitazawa *et al.* 1991; Gong *et al.* 1995) and that the activation of MLCP is linked to a decrease in Ca^{2+} sensitivity (Wu *et al.* 1996; Lee *et al.* 1997).

Smooth muscle MLCP has been isolated and cloned from chicken gizzard and pig bladder (Alessi *et al.* 1992; Shimizu *et al.* 1994; Shirazi *et al.* 1994). MLCP is a type 1 protein phosphatase (Cohen, 1989; Okubo *et al.* 1993) and is composed of three subunits: a catalytic subunit of 38 kDa (PP1c) and two regulatory subunits of 110–130 kDa (referred to as M110 for the rat isoform and M130 for the chicken isoform) and 20 kDa (M20) (Chen *et al.* 1994; Shimizu *et al.* 1994; Haystead *et al.* 1995). The major activity towards MLC in smooth muscle is thought to be due to the heterotrimeric holoenzyme (Hartshorne *et al.* 1998). M130 has been shown to perform two major regulatory functions: one is to target the phosphatase to myosin (Shimizu *et al.* 1994; Ichikawa *et al.* 1996*a*; Johnson *et al.* 1996; Hirano *et al.* 1997) and the other is to modulate catalytic activity depending on its phosphorylation state (Trinkle-Mulcahy *et al.* 1995; Ichikawa *et al.* 1996*b*; Kimura *et al.* 1996). The former function resides on an NH_2-terminal part of M130 (Okubo *et al.* 1993; Haystead *et al.* 1995; Ichikawa *et al.* 1996*a*; Johnson *et al.* 1996; Hirano *et al.* 1997). NH_2-terminal fragments of M130 have been shown to bind to myosin, interact with PP1c and substrate (phosphorylated MLC) and activate PP1c activity towards MLC (Shimizu *et al.* 1994; Ichikawa *et al.* 1996*a*; Johnson *et al.* 1996; Hirano *et al.* 1997). A region of M130 comprising residues 1–38 is essential for PP1c binding (Johnson *et al.* 1996; Hirano *et al.* 1997), and an ankyrin repeat structure (Shimizu *et al.* 1994) has been suggested to contain a weaker second binding site for PP1c and a binding site for MLC (Hirano *et al.* 1997). Activation of PP1c activity towards MLC requires both sites (Johnson *et al.* 1996; Hirano *et al.* 1997), but it has been suggested that an additional sequence of M130, a region containing an acidic amino acid cluster (Shimizu *et al.* 1994), is also necessary for the activation (Hirano *et al.* 1997).

In spite of these numerous *in vitro* studies using cell-free systems, there have been only a few reports describing the effect of M130 on smooth muscle contraction (Haystead *et al.* 1995; Gailly *et al.* 1996). These experiments indicated that M110 fragments stimulated PP1c activity. However, it should be noted that in these experiments the endogenous phosphatases were inhibited irreversibly by the phosphatase inhibitor microcystin (Honkanen *et al.* 1990; MacKintosh *et al.* 1995), and subsequently the effects on the relaxation rate of permeabilized fibres of exogenously added NH_2-terminal M110 fragments in combination with the purified PP1c were investigated. In the present study, we investigated the effects of exogenously added M130 fragments on the contraction of Triton X-100-permeabilized smooth muscle fibre preparations from porcine renal artery. We determined the MLC phosphorylation level and the contraction amplitude of the permeabilized smooth muscle fibres using a series of NH_2-terminal fragments of chicken gizzard M130, since M130 is highly conserved among human, rat and chicken (Hartshorne *et al.* 1998), and a porcine homologue has not been obtained. We found that exogenously added M130 fragments increased the Ca^{2+} sensitivity of the contractile apparatus. We suggest that this increase in Ca^{2+} sensitivity is due to inhibition of the endogenous MLCP, since MLC phosphorylation was also increased by M130 fragments at a constant $[Ca^{2+}]_i$ and the relaxation rate was reduced. The specific M130 domain responsible for this increase in Ca^{2+} sensitivity was the NH_2-terminal M130 fragment (residues 304–374) containing the acidic amino acid cluster.

METHODS

Materials

Oligonucleotides were synthesized by Sawady Technology (Tokyo, Japan) or Hokkaido System Science (Sapporo, Japan). Deoxyribonucleoside triphosphates (dATP, dCTP, dTTP, dGTP) were purchased from Takara (Tokyo, Japan). The expression vectors (pQE vectors) for hexahistidine-tagged proteins were purchased from Qiagen (Hilden, Germany). Mouse monoclonal anti-MLC (20 kDa) antibody, horseradish peroxidase-conjugated goat anti-mouse IgM antibody, creatine phosphate kinase, wortmannin, poly-L-glutamate (molecular weight, 2000–15 000), poly-L-aspartate (molecular weight, 5000–15 000) and low molecular weight heparin (approximate molecular weight, 3000) were purchased from Sigma. Calmodulin was purchased from Seikagaku Kogyo (Tokyo, Japan). Triton X-100 was purchased from Katayama Chemicals (Osaka, Japan).

Preparation of mutant proteins of the chicken gizzard M130

The NH_2-terminal fragments of the 130 kDa regulatory subunit (M130) of chicken gizzard myosin phosphatase were expressed as hexahistidine-tagged recombinant proteins using pQE expression vectors. *Escherichia coli* strain JM109 or M15[pREP4] (Qiagen) was used as a bacterial host for expression. Plasmids for the expression of the fragments corresponding to amino acid residues 1–296 ($M130^{1\text{-}296}$), 1–374 ($M130^{1\text{-}374}$), 1–633 ($M130^{1\text{-}633}$) and 304–511 ($M130^{304\text{-}511}$) have been described previously (Fig. 1) (Hirano *et al.* 1997). cDNAs for the other fragments ($M130^{44\text{-}633}$ and $M130^{297\text{-}374}$) were obtained by PCR amplification with either pQE-$M130^{1\text{-}374}$ or pQE-$M130^{1\text{-}633}$ as template DNA (Fig. 1). LA Taq DNA polymerase (Takara) was used for the PCR reaction. The sense and antisense primers were designed to contain *Bam*HI and *Sal*I sites, respectively, to enable ligation of the PCR products to the vector plasmids. The *Bam*HI- and *Sal*I-digested PCR products were ligated to the *Bam*HI- and *Sal*I-digested pQE31 vector using T4 ligase (DNA Ligation kit ver.2, Takara).

The expression of M130 fragments in *E. coli* was as described previously (Hirano *et al.* 1997). Purification of expressed protein was performed according to the manufacturer's instructions (Qiagen) with minor modifications. In brief, the bacterial pellet was resuspended in sonication buffer (50 mM sodium phosphate, 300 mM NaCl, pH 8·0) and homogenized with an ultrasonic disrupter (UD-201, Tomy, Tokyo, Japan). The homogenate was centrifuged at 25 000 *g* for 10 min at 4 °C, and the supernatant obtained was mixed for 1 h with nickel–nitrilotriacetic acid–agarose resin (Qiagen) equilibrated with sonication buffer. The resin was loaded onto a column and washed extensively in sonication buffer and then in wash buffer (50 mM sodium phosphate, 300 mM NaCl, 10% glycerol, pH 6·0) until the absorbance of the eluate at

280 nm from each of the washes was less than 0·01. Then the resin was washed with three volumes of wash buffer containing 50 mM imidazole. The histidine-tagged recombinant proteins were eluted in wash buffer containing 100 mM imidazole. Every fraction of the eluate was evaluated by SDS-PAGE. Fractions of greater than 70% purity were pooled and dialysed against 100 mM potassium methanesulphonate and 20 mM Tris-maleate (pH 7·0). The dialysate was cleared by centrifugation at 11 000 *g* at 4 °C for 10 min and concentrated using Centricon 10 (Amicon, Tokyo, Japan).

Preparation of porcine renal artery

Fresh kidneys from pigs of either sex were obtained from a local slaughterhouse. They were brought back to the laboratory in pre-aerated physiological salt solution (mM: NaCl, 123; KCl, 4·7; $NaHCO_3$, 15·5; KH_2PO_4, 1·2; $MgCl_2$, 1·2; $CaCl_2$, 1·25; and D-glucose, 11·5). The kidney was then cut open and the distal portions of the interlobular arteries were isolated. Arterial segments with an interior diameter of 200–250 μm were chosen. The fat and adventitia were mechanically removed under a binocular microscope. The segments were then cut into 500 μm wide vascular rings. The tissue and arterial segments were kept in physiological salt solution aerated with 95% O_2 and 5% CO_2 during all preparative procedures.

Permeabilization and force measurements

Arterial rings thus obtained were permeabilized with 1% Triton X-100 in Ca^{2+}-free cytoplasmic substitution solution (CSS (mM): EGTA, 10; potassium methanesulphonate, 100; $MgCl_2$, 3·38; Na_2ATP, 2·2; creatine phosphate, 10; and Tris-maleate, 20; pH 6·8) at 24–25 °C for 30 min. Measurement of isometric force was performed at 24–25 °C as described previously (Nishimura *et al.* 1988). Briefly, the tissue was mounted onto two tungsten wires bathed in wells filled with Ca^{2+}-free CSS on a plate, by passing the tungsten wires through the lumen of the arterial ring. One of the wires was fixed and the other was connected to a force transducer (U gauge, Minebea, Japan). The tissue was then stretched to two times its resting diameter, and was allowed to relax completely in Ca^{2+}-free CSS for 30 min. The extent of force development was expressed as a percentage, assigning values of 0 and 100% to the force in Ca^{2+}-free CSS (resting state) and 10 μM Ca^{2+} CSS (maximum contraction), respectively. The Ca^{2+} CSS containing the indicated concentration of free Ca^{2+} was prepared by adding an appropriate amount of $CaCl_2$, using the EGTA–Ca^{2+} binding constant of 10^6 M^{-1} (Saida & Nonomura, 1978). All solutions used for force measurement of permeabilized fibres were supplemented with 2 μM calmodulin and 50 U ml^{-1} creatine phosphate kinase.

The fragments of M130 were applied directly in CSS. Tissues treated with $M130^{1\text{-}633}$ or $M130^{44\text{-}633}$ were incubated in CSS containing 3 μM recombinant proteins at 4 °C for 3 h before force measurements (see Fig. 2 for determination of incubation time). In control experiments for this protocol, tissues were treated in the same way except that the protein solution was replaced with an equal volume of the dialysis buffer. The $[Ca^{2+}]_i$–force relationship of the Ca^{2+}-induced contraction obtained after a 3 h incubation in the vehicle-containing CSS did not differ from that obtained without the 3 h incubation (data not shown).

Measurement of MLC phosphorylation

The extent of MLC phosphorylation in permeabilized fibres was determined using the urea–glycerol gel electrophoresis technique (Persechini *et al.* 1986), followed by immunoblot detection with a specific mouse monoclonal anti-MLC antibody. Arterial ring preparations were obtained, permeabilized and treated in a similar way as described for the force study, except that the tissues were not attached to tungsten wires. At the indicated times, arterial rings were transferred into 90% acetone, 10% trichloroacetic acid and 10 mM dithiothreitol (DTT) pre-chilled at −80 °C to stop the reaction. Tissues were then washed extensively and stored in acetone containing 10 mM DTT at −80 °C. After the tissue had been dried to remove acetone, it was extracted in sample buffer (8 M urea, 20 mM Tris-base, 23 mM glycine, 0·004% Bromophenol Blue and 10 mM DTT) at room temperature for 1 h. The supernatant was subjected to electrophoresis on a 10% polyacrylamide, 40% glycerol gel, followed by transfer onto polyvinylidene difluoride membrane (BioRad, Hercules, CA, USA) in 10 mM Na_2HPO_4 (pH 7·6). The 20 kDa MLC, in both unphosphorylated and phosphorylated forms, was detected by a specific anti-MLC antibody (× 200 dilution), and a horseradish peroxidase-conjugated secondary antibody (× 1000 dilution). The immune complex was detected using the enhanced chemiluminescence technique (ECL plus kit; Amersham, Buckinghamshire, UK). X-OMAT AR film (Kodak, Rochester, NY, USA) was used to detect light emission. After scanning the X-ray film on an Epson colour scanner GT-9500, the density of unphosphorylated and phosphorylated

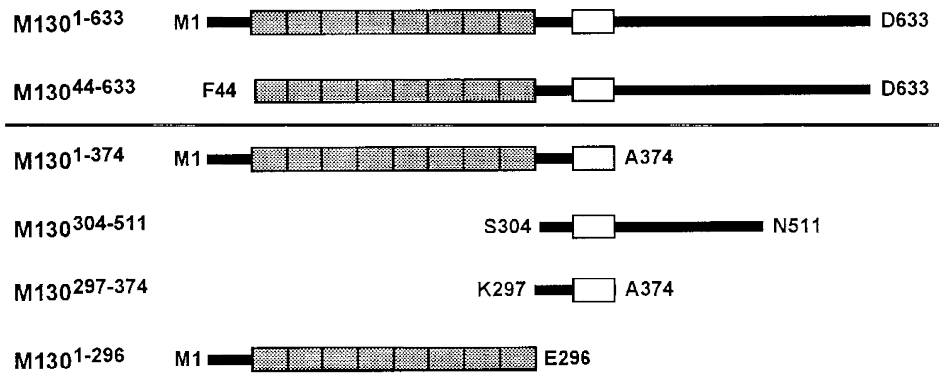

Figure 1. Schematic representation of the M130 fragments

The NH_2- and COOH-terminal residues are indicated by the single letter amino acid codes and the abbreviation used for each fragment is given. The shaded box area indicates the 8 ankyrin repeats, and the open box area is the acidic amino acid cluster (Shimizu *et al.* 1994).

MLCs was determined by Gel Plotting Macros of the NIH image version 1.61 (National Institutes of Health, USA). The percentage of the phosphorylated form in total MLC (sum of unphosphorylated and phosphorylated forms) was calculated to indicate the extent of MLC phosphorylation.

Other methods

Nucleotide sequences of the expression plasmids were determined with the dye-termination method on an ABI Prism 310 automated sequencer (Applied Biosystem, Foster City, CA, USA). The sequence data were analysed with the Wisconsin Sequence Analysis Package (Genetic Computer Group, Madison, WI, USA). SDS–PAGE and the immunoblot technique were as described (Lemmli, 1970; Towbin *et al.* 1979). The concentration of protein was determined by the Bradford method (Bradford, 1976) with bovine serum albumin as the standard (Pierce, Rockford, IL, USA).

Data analysis

The EC_{50} value, the concentration required to induce a force of 50% of the maximum response, was determined by fitting the concentration–response curves to a four-parameter logistic model (De Lean *et al.* 1978). The data are expressed as means ± S.E.M. Student's t test was used to determine statistically significant differences. $P < 0{\cdot}05$ was considered to be of statistical significance.

RESULTS

Effect of M130 fragments on Ca^{2+} sensitivity in permeabilized porcine renal artery

In the Triton X-100-permeabilized porcine renal artery, a stepwise increment of Ca^{2+} concentration caused a stepwise increase in force. In the presence of 2 μM calmodulin, force development was observed at Ca^{2+} concentrations higher than 180 nM. The maximum force development was obtained at 1 μM Ca^{2+}; there was no further force development above 1 μM Ca^{2+}. Therefore, the level of force obtained with 10 μM Ca^{2+} was assigned as 100%. Incubating permeabilized fibres in CSS containing dialysis buffer for 1, 2 and 3 h (for the control experiment) did not shift the $[Ca^{2+}]_i$–force curves (data not shown). Thus, Fig. 2 shows the control $[Ca^{2+}]_i$–force relationship obtained in fibres treated with control solution for 3 h. The concentration of Ca^{2+} required to obtain half the maximal force development (EC_{50}) was 329·6 ± 12·1 nM ($n = 4$) (Fig. 2).

When $M130^{1\text{-}633}$ was applied in 180 nM Ca^{2+} CSS, there was no further development of force (data not shown). However, in permeabilized fibres treated with 3 μM $M130^{1\text{-}633}$ in CSS at 4 °C for a longer period, the Ca^{2+}-induced contraction was augmented and the $[Ca^{2+}]_i$–force relationship curve shifted to the left (compared with control), depending on the length of the treatment (Fig. 2). The EC_{50} values for Ca^{2+} were significantly decreased to 227·8 ± 7·8, 191·7 ± 10·7 and 144·5 ± 31·2 nM ($n = 3$–4, $P < 0{\cdot}01$) by 1, 2 and 3 h treatment, respectively. Following treatment of the permeabilized fibres with $M130^{1\text{-}633}$, this enhancement of Ca^{2+}-induced contraction was observed even in the absence of M130 fragments in the bathing buffer. Similarly, treating the permeabilized fibres with 3 μM $M130^{44\text{-}633}$ in CSS at 4 °C for 3 h caused a leftward shift of the Ca^{2+}–force curves. The EC_{50} value obtained in the $M130^{44\text{-}633}$-treated fibres was 163·1 ± 5·6 nM ($n = 4$, $P < 0{\cdot}01$) and did not differ significantly from that obtained with $M130^{1\text{-}633}$. Thus, $M130^{44\text{-}633}$ had a similar effect to that seen with $M130^{1\text{-}633}$.

$M130^{1\text{-}374}$, $M130^{304\text{-}511}$ and $M130^{297\text{-}374}$ were effective in augmenting the Ca^{2+}-induced contraction, but without pretreatment (Fig. 3*A*, *B* and *C*). When these fragments were applied in 180 nM Ca^{2+} CSS, there was an instant development of force. Application of 3 μM $M130^{1\text{-}374}$, $M130^{304\text{-}511}$ or $M130^{297\text{-}374}$ caused 81·7, 70·7 and 34·7% force development, respectively. The effects of these M130 fragments were concentration dependent. Figure 3*F* shows a concentration–response curve for the $M130^{1\text{-}374}$-induced contraction in 180 nM Ca^{2+} CSS. The fragment had enhancing effects at concentrations above 0·5 μM, and maximal enhancement was obtained at 3 μM. The concentration of $M130^{1\text{-}374}$ required to induce half the maximal enhancement was 1·4 ± 0·2 μM ($n = 3$). The $[Ca^{2+}]_i$–force relationships of the Ca^{2+}-induced contractions obtained in the presence of these fragments were shifted leftwards (Fig. 4). The EC_{50} values for Ca^{2+} obtained in the presence of 3 μM $M130^{1\text{-}374}$,

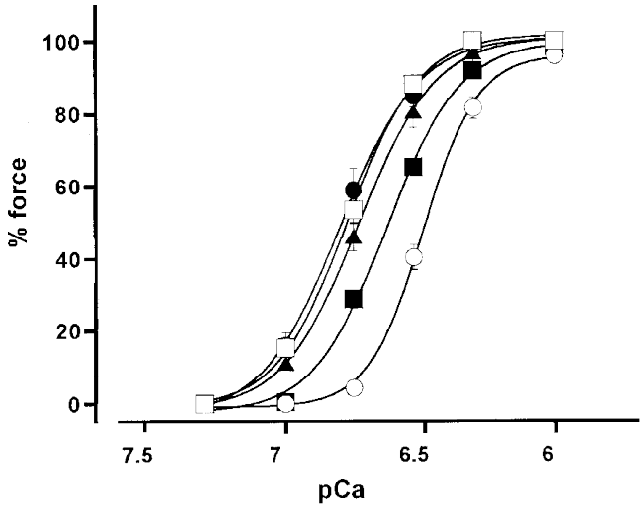

Figure 2. Effects of $M130^{1\text{-}633}$ and $M130^{44\text{-}633}$ on the $[Ca^{2+}]_i$–force relationship of the Ca^{2+}-induced contraction in 1% Triton X-100-permeabilized porcine renal artery

The permeabilized fibres were pretreated with 3 μM $M130^{1\text{-}633}$ for 1 (■), 2 (▲) and 3 h (●) or 3 μM $M130^{44\text{-}633}$ for 3 h (□) at 4 °C in Ca^{2+}-free cytoplasmic substitution solution (CSS) (see Methods for composition). Then, the fibres were mounted and connected to a force transducer in the buffer without M130 fragments, and contraction was initiated by incrementing the Ca^{2+} concentration. The $[Ca^{2+}]_i$–force relationship curve of the control contraction (○) was obtained in permeabilized fibres treated with vehicle (dialysis buffer) for 3 h at 4 °C. Force development is expressed as a percentage of that obtained with 10 μM Ca^{2+}. Data are means ± S.E.M. ($n = 3$–4).

$M130^{304-511}$ and $M130^{297-374}$ were $65{\cdot}2 \pm 10{\cdot}8$, $72{\cdot}3 \pm 13{\cdot}4$ and $180{\cdot}1 \pm 13{\cdot}5$ nM ($n = 3$, $P < 0{\cdot}01$), respectively.

In contrast, 3 μM $M130^{1-296}$ did not induce a contraction in 180 nM Ca^{2+} CSS (Fig. 3*D*). Higher concentrations of $M130^{1-296}$, up to 5 μM, had no effect on the Ca^{2+}-induced contraction (data not shown). The $[Ca^{2+}]_i$–force relationship obtained in the presence of 3 μM $M130^{1-296}$ overlapped the control relationship obtained without M130 fragments (Fig. 4). The EC_{50} value obtained in the presence of $M130^{1-296}$ was $340{\cdot}3 \pm 22{\cdot}2$ nM ($n = 3$). This value did not significantly differ from the control value ($351{\cdot}4 \pm 26{\cdot}4$ nM). Pretreatment of permeabilized fibres with 3 μM $M130^{1-296}$ for 3 h had no effect on the Ca^{2+}-induced contraction or on its $[Ca^{2+}]_i$–force relationship curve (data not shown).

Among the NH_2-terminal fragments of M130 evaluated in the present study, $M130^{297-374}$ was the shortest fragment to induce augmentation of the Ca^{2+}-induced contraction in Triton X-100-permeabilized porcine renal artery. Since $M130^{297-374}$ contains a cluster of acidic amino acids (Shimizu *et al.* 1994), there was the possibility that negative charge and not the specific structure of the M130 fragments was linked to the augmentation of the Ca^{2+}-induced contraction. Thus, we examined the effects of poly-L-glutamate (molecular weight, 2000–15 000), poly-L-aspartate (molecular weight,

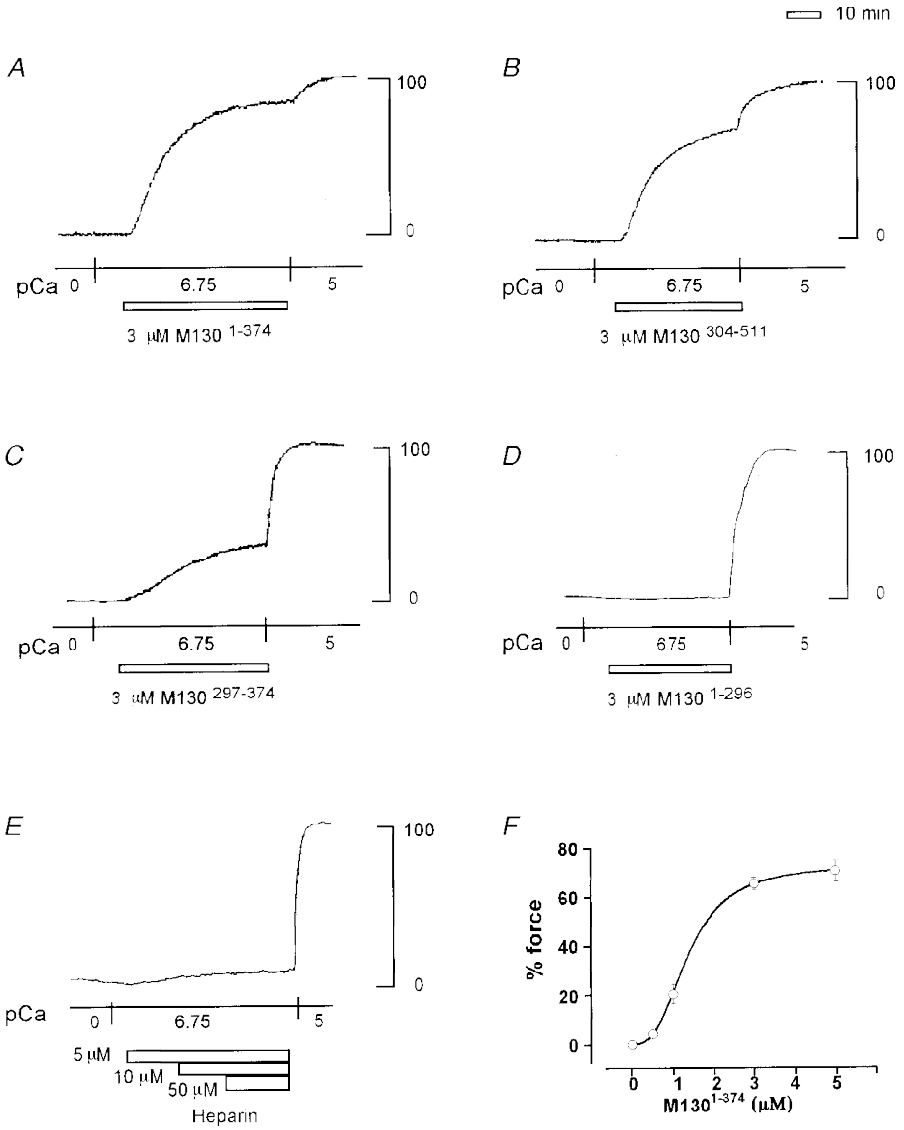

Figure 3. Effect of $M130^{1-374}$, $M130^{304-511}$, $M130^{297-374}$, $M130^{1-296}$ and heparin on contraction in 1% Triton X-100-permeabilized porcine renal artery

A–E, representative recordings showing the effect of 3 μM $M130^{1-374}$ (*A*), 3 μM $M130^{304-511}$ (*B*), 3 μM $M130^{297-374}$ (*C*), 3 μM $M130^{1-296}$ (*D*) and 5, 10 and 50 μM heparin (*E*) on the force development in 180 nM Ca^{2+} CSS. *F*, concentration–response curve for the contraction induced by $M130^{1-374}$ in 180 nM Ca^{2+} CSS in 1% Triton X-100-permeabilized porcine renal artery. Force development is expressed as a percentage of that obtained with 10 μM Ca^{2+}. Data are means ± S.E.M. ($n = 3$).

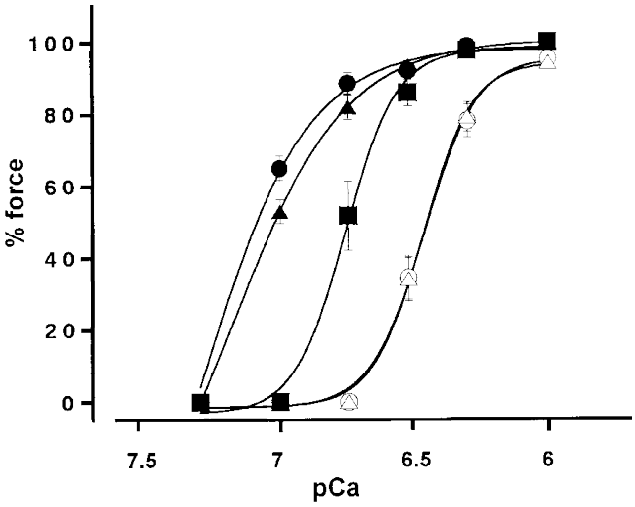

Figure 4. $[Ca^{2+}]_i$–force relationship curves for contractions induced by incrementing Ca^{2+} levels in the absence and presence of M130 fragments

○, control; △, 3 μM $M130^{1-296}$; ■, 3 μM $M130^{297-374}$; ▲, 3 μM $M130^{304-511}$; and ●, 3 μM $M130^{1-374}$. Force development is expressed as a percentage of that obtained with 10 μM Ca^{2+}. Data are means ± S.E.M. ($n = 3$–4).

5000–15000) and low molecular weight heparin (approximate molecular weight, 3000) on the Ca^{2+}-induced contraction. Neither poly-L-glutamate nor poly-L-aspartate, up to 5 μM, induced force in either 180 or 300 nM Ca^{2+} CSS (data not shown). The multiple negative charge carrier heparin had no effect up to 1 μM, although 5 μM heparin induced a small but significant development of force in 180 nM Ca^{2+} CSS. However, the extent of force development induced by 5 μM heparin in 180 nM Ca^{2+} CSS was 5%, which was much lower than that obtained with $M130^{1-374}$

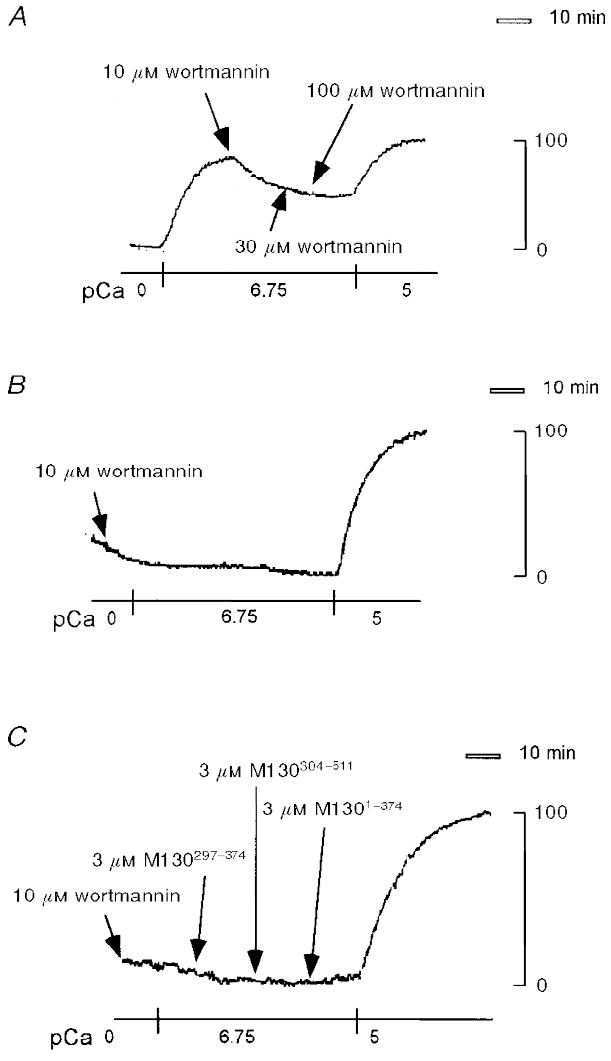

Figure 5. Effects of wortmannin on the enhancement of Ca^{2+}-induced contraction by M130 fragments in 1% Triton X-100-permeabilized porcine renal artery

A and *B*, permeabilized fibres were treated with 3 μM $M130^{1-633}$ in CSS at 4 °C for 3 h, and 10, 30 and 100 μM wortmannin was applied at the times indicated by arrows after the 180 nM Ca^{2+}-induced contraction reached a steady state (*A*), or 10 μM wortmannin was applied 5 min before the induction of contraction by 180 nM Ca^{2+} CSS (*B*). *C*, after treatment with 10 μM wortmannin for 5 min in CSS and exposure to 180 nM Ca^{2+} CSS, permeabilized fibres were consecutively stimulated with 3 μM $M130^{297-374}$, 3 μM $M130^{304-511}$ and 3 μM $M130^{1-374}$, at the times indicated by arrows. These are representative traces of three independent experiments, which yielded similar results.

(Fig. 3*E*). Further increments in the concentration of heparin up to 50 μM did not cause further force development.

Effect of wortmannin on the Ca^{2+} sensitization induced by M130 mutants

Figure 5*A* and *B* shows the effect of wortmannin on the 180 nM Ca^{2+}-induced contractions of permeabilized fibres treated with 3 μM $M130^{1-633}$ at 4 °C for 3 h. Wortmannin was used as an inhibitor of MLCK because only two kinases, MLCK and phosphatidyl inositol 3-kinase, are reported to be the major target kinases of wortmannin (Yano *et al.* 1993). When applied during the steady state of the 180 nM Ca^{2+}-induced contraction, 10 μM wortmannin relaxed contraction by 39% (Fig. 5*A*). However, the inhibition was partial even with 30 and 100 μM wortmannin. In contrast, when 10 μM wortmannin was applied 5 min before and during the application of 180 nM Ca^{2+}, force development was completely inhibited (Fig. 5*B*). Similarly, application of 10 μM wortmannin before the induction of contraction completely inhibited the subsequent force development induced by 3 μM $M130^{1-374}$, $M130^{304-511}$ and $M130^{297-374}$ in 180 nM Ca^{2+} CSS (Fig. 5*C*).

Effect of $M130^{1-374}$ on relaxation in permeabilized porcine renal artery

Figure 6 shows the effect of $M130^{1-374}$ on the relaxation induced by exposure to Ca^{2+}-free CSS in the permeabilized porcine renal artery. The fibres were contracted by 10 μM Ca^{2+} CSS, and then relaxation was induced by exposure to Ca^{2+}-free CSS, in either the presence or the absence of 3 μM $M130^{1-374}$. $M130^{1-374}$ was applied 5 min before exposure to the Ca^{2+}-free CSS, when the precontraction induced by 10 μM Ca^{2+} was in the sustained phase. There was no further force development by the application of $M130^{1-374}$. The relaxing solution contained 10 μM wortmannin to inhibit any MLCK activity in the Ca^{2+}-free CSS. Thus, the relaxation rate was considered to represent myosin phosphatase activity. As shown in Fig. 6, $M130^{1-374}$ significantly slowed relaxation rate. The time to cause a 50% reduction of force obtained in the presence of $M130^{1-374}$ (510·0 ± 51·4 s, $n = 4$) was significantly ($P < 0·001$) longer than that obtained in its absence (control relaxation, 273·6 ± 13·5 s, $n = 4$).

MLC phosphorylation during the $M130^{1-374}$-induced enhancement of contractions

The effects of the $M130^{1-374}$ fragment on the level of MLC phosphorylation and the relationship between the extent of MLC phosphorylation and developed force were examined. The level of MLC phosphorylation was determined in arterial tissues under the unloaded condition, while force measurement was performed under the isometrically loaded condition. The extent of MLC phosphorylation with no developed tension (0% tension) obtained in the Ca^{2+}-free CSS was 10·9 ± 2·7% ($n = 4$) (Fig. 7*A*, column 1). During the steady-state contractions induced by 300 nM, 1 μM and 10 μM Ca^{2+}, the extent of MLC phosphorylation significantly increased to 22·4 ± 4·0% ($n = 4$, $P < 0·05$), 41·1 ± 6·4% ($n = 3$, $P < 0·005$), and 64·3 ± 1·9% ($n = 3$, $P < 0·001$), and force developed to 34·5 ± 6·2, 95·5 ± 2·9 and 100% ($n = 3$), respectively (Fig. 7*A*, columns 2, 4 and 5, respectively). Addition of 3 μM $M130^{1-374}$ in 300 nM Ca^{2+} CSS induced a further force development (92·2 ± 2·0%, $n = 3$) associated with a significant increase in MLC phosphorylation (35·7 ± 4·2% at 30 min after the induction of contraction; $n = 4$, $P < 0·01$) (Fig. 7*A*, column 3). The relationship between the level of MLC phosphorylation and the extent of force obtained with 300 nM Ca^{2+} in the presence of 3 μM $M130^{1-374}$ was similar to that obtained with 1 μM Ca^{2+} in the absence of $M130^{1-374}$ (Fig. 7*A*). This is clearly demonstrated in Fig. 7*B*. The control phosphorylation–force curve was reconstructed from the values of MLC phosphorylation and force shown in Fig. 7*A*. The phosphorylation–force relationship obtained with 300 nM Ca^{2+} in the presence of $M130^{1-374}$ fitted the control curve.

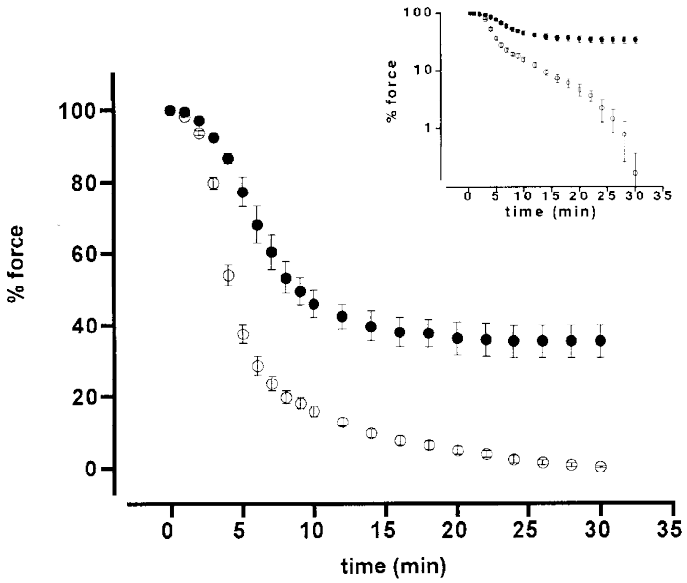

Figure 6. Effect of $M130^{1-374}$ on relaxation in 1% Triton X-100-permeabilized porcine renal artery
The permeabilized fibres were contracted with 10 μM Ca^{2+} CSS, and then relaxed by exposure to Ca^{2+}-free CSS containing 10 μM wortmannin in either the presence (●) or the absence (○) of 3 μM $M130^{1-374}$. $M130^{1-374}$ was applied 5 min prior to exposure to Ca^{2+}-free CSS. Force development is expressed as a percentage of that obtained with 10 μM Ca^{2+}. Data are means ± S.E.M. ($n = 4$). Inset, a semilog plot of the same data, showing a decrease of force regression during relaxation for fibres in the presence of 3 μM $M130^{1-374}$ (■) compared with that in control fibres (○).

DISCUSSION

In the present study, we investigated the effects of a series of NH_2-terminal fragments of chicken M130 on the Ca^{2+}-induced contractions of permeabilized porcine renal artery. The major findings are as follows. (1) The NH_2-terminal fragments of M130 induced contractions at a constant $[Ca^{2+}]_i$ and shifted the $[Ca^{2+}]_i$–force relationship to the left. (2) This effect was completely abolished by deleting the amino acid sequence 304–374. (3) The contraction induced by $M130^{1\text{-}374}$, the most potent construct, was accompanied by an increase in MLC phosphorylation. (4) The relationship between the level of MLC phosphorylation and force remained unchanged, irrespective of the presence or absence of $M130^{1\text{-}374}$. (5) Wortmannin was more effective in inhibiting Ca^{2+} sensitization by the NH_2-terminal fragments when applied before contraction was initiated, compared with the addition during steady-state contraction. (6) The rate of relaxation was decreased by treatment with $M130^{1\text{-}374}$. Based on these findings, we propose that the NH_2-terminal fragments of M130 could inhibit endogenous MLCP activity. Although the mechanism is still speculative, this is the first report showing that the NH_2-terminal fragments of M130 increase MLC phosphorylation and Ca^{2+} sensitivity of permeabilized smooth muscle preparations.

The increases in Ca^{2+} sensitivity induced by the M130 fragments are clearly demonstrated in Figs 2, 3 and 4. Because $[Ca^{2+}]_i$ was clamped in the permeabilized preparation, force developed at a constant level of Ca^{2+}, thus indicating an increase in the Ca^{2+} sensitivity of the contractile apparatus. This increase in Ca^{2+} sensitivity was a marked effect (as opposed to a subtle change), because the M130 fragments induced almost 90% of the maximal contraction at a Ca^{2+} concentration of 180 nM, which alone caused no contraction (Fig. 3*A* and *B*). The extent of the change was also noted by the quantitative evaluation of Ca^{2+} sensitivity, in which a marked leftward shift of the $[Ca^{2+}]_i$–force curve induced by the M130 fragments was observed (Figs 2 and 4). These results indicate that the M130 fragments caused an increase in Ca^{2+} sensitivity. However, there is the possibility that the histidine tag or other possible contaminating bacterial proteins might be responsible for the apparent Ca^{2+}-sensitizing effects (Buning

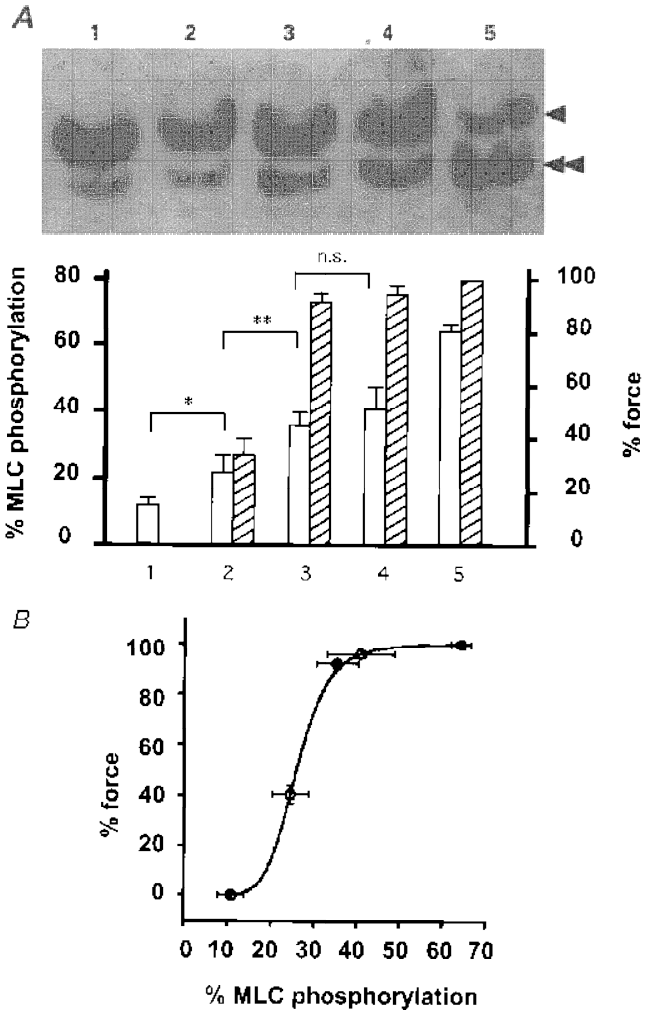

Figure 7. Effects of $M130^{1\text{-}374}$ on MLC phosphorylation and on the relationship between MLC phosphorylation and force in 1% Triton X-100-permeabilized porcine renal artery

A, representative photograph of the MLC immunoblot (upper panel) and summary (lower panel) of MLC phosphorylation and force obtained by 30 min incubation in CSS (1), 300 nM Ca^{2+} (2), 300 nM Ca^{2+} plus 3 μM $M130^{1\text{-}374}$ (3), 1 μM Ca^{2+} (4) and 10 μM Ca^{2+} (5). Single arrowhead, unphosphorylated MLC; double arrowhead, monophosphorylated MLC. □, MLC phosphorylation; ▨, force. The level of phosphorylation is expressed as a percentage of phosphorylated MLC in the total MLC (as described in Methods). Force development is expressed as a percentage of that obtained with 10 μM Ca^{2+}. Values of force obtained in the absence of $M130^{1\text{-}374}$ (columns 1, 2, 4 and 5) are from Fig. 4. Data are means ± S.E.M. ($n = 3$–4). * $P < 0{\cdot}05$; ** $P < 0{\cdot}01$; n.s., not significantly different. *B*, MLC phosphorylation–force relationship curve reconstructed from data shown in *A*. ○, phosphorylation–force relationship obtained with 0, 300 nM, 1 μM and 10 μM Ca^{2+} in the absence of $M130^{1\text{-}374}$. ●, phosphorylation–force relationship obtained with 300 nM Ca^{2+} in the presence of 3 μM $M130^{1\text{-}374}$.

et al. 1996). This possibility may be ruled out by the observation that $M130^{1-296}$ was inert even at concentrations up to 5 μM, with or without 3 h treatment (Fig. 3*D*). Thus, we conclude that the M130 fragments themselves induce an increase in Ca^{2+} sensitivity.

Since the Ca^{2+}-sensitizing effect is due to the NH_2-terminal fragments of M130, we attempted to identify the region responsible for this effect by using a series of truncated fragments. The Ca^{2+}-sensitizing effect could not be abolished by deletion of amino acids 1–43 ($M130^{44-633}$) or by deletion of the ankyrin repeats ($M130^{304-511}$, $M130^{297-374}$; Figs 1–4), both of which are important for the activation of PP1c (Johnson *et al.* 1996; Hirano *et al.* 1997; Hartshorne *et al.* 1998). Also, deletion of the amino acid sequence 375–633 ($M130^{1-374}$) did not affect the Ca^{2+}-sensitizing effect. However, the Ca^{2+}-sensitizing effect was completely abolished by deletion of amino acids 304–374 ($M130^{1-296}$; Fig. 3*D*). We thus conclude that an essential sequence required for the Ca^{2+}-sensitizing effect may be located within residues 304 to 374. One characteristic of this area is a cluster of acidic amino acids (Shimizu *et al.* 1994).

In contrast to the present conclusion, previous studies indicated that the NH_2-terminal fragments of rat M110, a rat homologue of M130, induced activation of PP1c in permeabilized rabbit portal vein (Haystead *et al.* 1995; Gailly *et al.* 1996). This discrepancy may have arisen for the following reasons. First, these authors investigated the effects of exogenously added NH_2-terminal M110 fragments in combination with purified PP1c on the relaxation rate of permeabilized smooth muscle fibres after the endogenous phosphatases had been inhibited by an irreversible phosphatase inhibitor, microcystin (Honkanen *et al.* 1990; MacKintosh *et al.* 1995). In contrast, we investigated the effects of exogenously added M130 fragments on the endogenous MLCP activity. Second, the NH_2-terminal M110 fragments ($M110^{1-309}$ and $M110^{39-309}$) used by others lack the acidic amino acid cluster that we suggest is responsible for the increase in Ca^{2+} sensitivity. Thus, the various reports are not necessarily in conflict, because $M130^{1-296}$ (present study) had no effect on Ca^{2+} sensitivity, and this corresponds to the $M110^{1-309}$ fragment used in the quoted studies. Third, the long constructs, e.g. $M130^{44-633}$ or $M130^{1-633}$, required 1–3 h incubation to influence Ca^{2+} sensitivity (Fig. 2). Although a long construct, $M110^{11-612}$, was used by Gailly *et al.* (1996), an effect on Ca^{2+} sensitivity was not described. This could be due to the requirement for a preincubation period for these large constructs to show an effect. The requirement for a longer incubation time with $M130^{1-633}$ and $M130^{44-633}$ can be simply explained by the suggestion that diffusion of these constructs to the target sites was hindered due to their larger molecular size. However, there is a possibility that longer constructs were slowly proteolysed during the incubation at 4 °C and only degradation products containing the acidic cluster were effective in enhancing Ca^{2+}-induced contraction.

In order to clarify the mechanism for the Ca^{2+}-sensitizing effect by the NH_2-terminal fragments of M130, we examined the level of MLC phosphorylation. As shown in Fig. 7, the contraction induced by $M130^{1-374}$ was accompanied by an increase in MLC phosphorylation. However, the relationship between the level of MLC phosphorylation and force remained unchanged, irrespective of the presence or absence of $M130^{1-374}$. It was thus indicated that the Ca^{2+}-sensitizing effect is due to an increase in MLC phosphorylation and not to other effects on the contractile apparatus (e.g. effect on cross-bridges or other regulatory components). Since $[Ca^{2+}]_i$ was kept constant in the permeabilized preparation, the activity of MLCK should remain constant. Thus, the increase in MLC phosphorylation was considered to be due to inhibition of myosin phosphatase by the M130 fragments. This is supported by the observation that the relaxation rate was decreased by $M130^{1-374}$ (Fig. 6). Since relaxation was induced in the presence of a MLCK inhibitor and in Ca^{2+}-free CSS, the rate of relaxation should reflect myosin phosphatase activity. Evidence consistent with this idea is that wortmannin was more effective in inhibiting the Ca^{2+} sensitization by the NH_2-terminal fragments when applied before the contraction was initiated, rather than after the contraction reached steady state.

A possible explanation for the effect of M130 fragments could be that the negatively charged acidic amino acid cluster inhibits myosin phosphatase in a non-specific manner. Charged compounds, either positive or negative, are known to modulate PP1c activity (Bollen & Stalmans, 1992). For example, positively charged spermine was shown to increase MLC phosphorylation and cause contraction in both β-escin- and Triton X-100-permeabilized guinea-pig ileum (Swärd *et al.* 1995). Similarly, heparin, a multiple negative charge carrier, was shown to bind to PP1c and inhibit or stimulate activity depending on the substrates used (Bollen & Stalmans, 1992). To exclude this possibility, we examined the effects of negatively charged compounds such as poly-L-glutamate, poly-L-aspartate and heparin on the Ca^{2+}-induced contractions of the permeabilized fibres. Among these compounds, only heparin produced a significant force, but this was much smaller than that seen with the M130 fragments. We thus consider that the inhibition of PP1c activity due to a non-specific charge effect is not responsible for the effect seen with the M130 fragments.

It is possible that amino acids 304–374 might act as an 'inhibitory domain' of M130 against PP1c. However, this region shows no similarity to the inhibitory regions of known PP1c inhibitors. It was noticed that the COOH-terminal part of M130, around the possible phosphorylation site (Ichikawa *et al.* 1996*b*), contains a region similar to the inhibitory domain of inhibitor-1 or the 32 kDa dopamine- and cAMP-regulated phosphoprotein (DARPP-32) (Hartshorne *et al.* 1998). Another possible explanation is that the inhibition of

myosin phosphatase by M130 fragments may be due to an alteration of subunit interactions of the holoenzyme. Arachidonic acid was shown to interact with MLCP, disrupt the subunit interactions and thereby inhibit MLCP (Gong *et al.* 1992). It is thus possible that MLCP activity could be inhibited when one or more of the subunit interactions important for the activation of PP1c activity towards myosin are hindered by exogenously added M130 fragments. In other words, exogenously added M130 fragments might behave as a dominant negative. This is consistent with a report that amino acids 297–374 in addition to the PP1c-binding site (amino acids 1–38) and ankyrin repeats (amino acids 39–286) are required for activation of MLCP activity towards myosin (Hirano *et al.* 1997). If this is the case, the effects of M130 fragments would be expected to be stoichiometric with the endogenous M130. In the rabbit portal vein, the concentration of M130 was estimated to be $1{\cdot}2 \pm 0{\cdot}3\ \mu$M (personal communication cited in Hartshorne *et al.* 1998). This value agrees with the concentration of $M130^{1\text{-}374}$ required to induce the half-maximum Ca^{2+}-sensitizing effect. M130 was shown to bind to both the catalytic subunit and myosin, and considered to target the catalytic subunit close to the substrate, i.e. myosin (Alessi *et al.* 1992; Shimizu *et al.* 1994). The activity of the catalytic subunit in the presence of M130 was greater with myosin as a substrate than with MLC (Ichikawa *et al.* 1996*a*). These results suggest that the interaction of M130 with myosin contributes to the regulation of MLCP activity. Thus, it is possible that exogenously added M130 fragments could inhibit the interaction of endogenous enzyme with myosin, and thereby inhibit phosphatase activity. These hypotheses are clearly speculative and further work is required to establish the molecular basis for the effect of the M130 fragments observed above.

In summary, the NH_2-terminal fragments of M130, a regulatory subunit of MLCP, caused an increase in the Ca^{2+} sensitivity of the contractile apparatus in porcine renal artery permeabilized with Triton X-100. This Ca^{2+} sensitization was accompanied by an increase in MLC phosphorylation. Thus, we consider that the increase in Ca^{2+} sensitivity induced by the NH_2-terminal fragments of M130 reflects an inhibition of the endogenous MLCP. A region essential for this Ca^{2+}-sensitizing effect is the amino acid sequence 304 to 374.

Alessi, D., MacDougall, L. K., Sola, M. M., Ikebe, M. & Cohen, P. (1992). The control of protein phosphatase-1 by targetting subunits. The major myosin phosphatase in avian smooth muscle is a novel form of protein phosphatase-1. *European Journal of Biochemistry* **210**, 1023–1035.

Bollen, M. & Stalmans, W. (1992). The structure, role, and regulation of type 1 protein phosphatases. *Critical Reviews in Biochemistry and Molecular Biology* **27**, 227–281.

Bradford, M. (1976). A rapid and sensitive method for the quantitation of microgram quantities of protein utilizing the principle of protein dye-binding. *Analytical Biochemistry* **72**, 248–254.

Buning, H., Gartner, U., von Schack, D., Baeuerle, P. A. & Zorbas, H. (1996). The histidine tail of recombinant DNA binding proteins may influence the quality of interaction with DNA. *Analytical Biochemistry* **234**, 227–230.

Chen, Y. H., Chen, M. X., Alessi, D. R., Campbell, D. G., Shanahan, C., Cohen, P. & Cohen, P. T. (1994). Molecular cloning of cDNA encoding the 110 kDa and 21 kDa regulatory subunits of smooth muscle protein phosphatase 1M. *FEBS Letters* **356**, 51–55.

Cohen, P. (1989). The structure and regulation of protein phosphatases. *Annual Review of Biochemistry* **58**, 453–508.

De Lean, A., Munson, P. J. & Rodbard, D. (1978). Simultaneous analysis of families of sigmoidal curves: application to bioassay, radioligand assay, and physiological dose-response curves. *American Journal of Physiology* **235**, E97–102.

Gailly, P., Wu, X., Haystead, T. A., Somlyo, A. P., Cohen, P. T., Cohen, P. & Somlyo, A. V. (1996). Regions of the 110-kDa regulatory subunit M110 required for regulation of myosin-light-chain-phosphatase activity in smooth muscle. *European Journal of Biochemistry* **239**, 326–332.

Gong, M. C., Fuglsang, A., Alessi, D., Kobayashi, S., Cohen, P., Somlyo, A. V. & Somlyo, A. P. (1992). Arachidonic acid inhibits myosin light chain phosphatase and sensitizes smooth muscle to calcium. *Journal of Biological Chemistry* **267**, 21492–21498.

Gong, M. C., Kinter, M. T., Somlyo, A. V. & Somlyo, A. P. (1995). Arachidonic acid and diacylglycerol release associated with inhibition of myosin light chain dephosphorylation in rabbit smooth muscle. *Journal of Physiology* **486**, 113–122.

Hartshorne, D. J. (1987). Biochemistry of the contractile process in smooth muscle. In *Physiology of the Gastrointestinal Tract,* ed. Johnson, L. R., pp. 423–482. Raven Press, New York.

Hartshorne, D. J., Ito, M. & Erdödi, F. (1998). Myosin light chain phosphatase: subunit composition, interactions and regulation. *Journal of Muscle Research and Cell Motility* **19**, 325–341.

Haystead, C. M., Gailly, P., Somlyo, A. P., Somlyo, A. V. & Haystead, T. A. (1995). Molecular cloning and functional expression of a recombinant 72.5 kDa fragment of the 110 kDa regulatory subunit of smooth muscle protein phosphatase 1M. *FEBS Letters* **377**, 123–127.

Hirano, K., Phan, B. C. & Hartshorne, D. J. (1997). Interactions of the subunits of smooth muscle myosin phosphatase. *Journal of Biological Chemistry* **272**, 3683–3688.

Honkanen, R. E., Zwiller, J., Moore, R. E., Daily, S. L., Khatra, B. S., Dukelow, M. & Boynton, A. L. (1990). Characterization of microcystin-LR, a potent inhibitor of type 1 and type 2A protein phosphatases. *Journal of Biological Chemistry* **265**, 19401–19404.

Ichikawa, K., Hirano, K., Ito, M., Tanaka, J., Nakano, T. & Hartshorne, D. J. (1996*a*). Interactions and properties of smooth muscle myosin phosphatase. *Biochemistry* **35**, 6313–6320.

Ichikawa, K., Ito, M. & Hartshorne, D. J. (1996*b*). Phosphorylation of the large subunit of myosin phosphatase and inhibition of phosphatase activity. *Journal of Biological Chemistry* **271**, 4733–4740.

Johnson, D. F., Moorhead, G., Caudwell, F. B., Cohen, P., Chen, Y. H., Chen, M. X. & Cohen, P. T. (1996). Identification of protein-phosphatase-1-binding domains on the glycogen and myofibrillar targetting subunits. *European Journal of Biochemistry* **239**, 317–325.

Kanaide, H. (1995). Cytosolic calcium concentration-force relation in vascular smooth muscle. In *Regulation of the Contractile Cycle in Smooth Muscle*, ed. Nakano, T. & Hartshorne, D. J., pp. 61–72. Springer-Verlag, Tokyo.

Kimura, K., Ito, M., Amano, M., Chihara, K., Fukata, Y., Nakafuku, M., Yamamori, B., Feng, J., Nakano, T., Okawa, K., Iwamatsu, A. & Kaibuchi, K. (1996). Regulation of myosin phosphatase by Rho and Rho-associated kinase (Rho-kinase). *Science* **273**, 245–248.

Kitazawa, T., Masuo, M. & Somlyo, A. P. (1991). G protein-mediated inhibition of myosin light-chain phosphatase in vascular smooth muscle. *Proceedings of the National Academy of Sciences of the USA* **88**, 9307–9310.

Lee, M. R., Li, L. & Kitazawa, T. (1997). Cyclic GMP causes Ca^{2+} desensitization in vascular smooth muscle by activating the myosin light chain phosphatase. *Journal of Biological Chemistry* **272**, 5063–5068.

Lemmli, U. K. (1970). Cleavage of structural proteins during the assembly of the head of bacteriophage T4. *Nature* **227**, 680–685.

MacKintosh, R. W., Dalby, K. N., Campbell, D. G., Cohen, P. T. W., Cohen, P. & MacKintosh, C. (1995). The cyanobacterial toxin microcystin binds covalently to cysteine-273 on protein phosphatase 1. *FEBS Letters* **371**, 236–240.

Morgan, J. P. & Morgan, K. G. (1984). Stimulus-specific patterns of intracellular calcium levels in smooth muscle of ferret portal vein. *Journal of Physiology* **73**, 673–699.

Nishimura, J., Kolber, M. & Van Breemen, C. (1988). Norepinephrine and GTP-γ-S increase myofilament Ca^{2+} sensitivity in α-toxin permeabilized arterial smooth muscle. *Biochemical and Biophysical Research Communications* **157**, 677–683.

Okubo, S., Erdödi, F., Ito, M., Ichikawa, K., Konishi, T., Nakano, T., Kawamura, T., Brautigan, D. L. & Hartshorne, D. J. (1993). Characterization of a myosin-bound phosphatase from smooth muscle. *Advances in Protein Phosphatases* **7**, 295–314.

Persechini, A., Kamm, K. E. & Stull, J. T. (1986). Different phosphorylated forms of myosin in contracting tracheal smooth muscle. *Journal of Biological Chemistry* **261**, 6293–6299.

Saida, K. & Nonomura, Y. (1978). Characteristics of Ca^{2+}- and Mg^{2+}-induced tension development in chemically skinned smooth muscle fibers. *Journal of General Physiology* **72**, 1–14.

Shimizu, H., Ito, M., Miyahara, M., Ichikawa, K., Okubo, S., Konishi, T., Naka, M., Tanaka, T., Hirano, K., Hartshorne, D. J. & Nakano, T. (1994). Characterization of the myosin-binding subunit of smooth muscle myosin phosphatase. *Journal of Biological Chemistry* **269**, 30407–30411.

Shirazi, A., Iizuka, K., Fadden, P., Mosse, C., Somlyo, A. P., Somlyo, A. V. & Haystead, T. A. (1994). Purification and characterization of the mammalian myosin light chain phosphatase holoenzyme. The differential effects of the holoenzyme and its subunits on smooth muscle. *Journal of Biological Chemistry* **269**, 31598–31606.

Somlyo, A. P., Kitazawa, T., Himpens, B., Matthijs, G., Horiuti, K., Kobayashi, S., Goldman, Y. E. & Somlyo, A. V. (1989). Modulation of Ca^{2+}-sensitivity and of the time course of contraction in smooth muscle: A major role of protein phosphatases? *Advances in Protein Phosphatases* **5**, 181–195.

Somlyo, A. P. & Somlyo, A. V. (1994). Signal transduction and regulation in smooth muscle. *Nature* **372**, 231–236.

Swärd, K., Pato, M. D., Nilsson, B. O., Nordström, I. & Hellstrand, P. (1995). Polyamines inhibit myosin phosphatase and increase LC20 phosphorylation and force in smooth muscle. *American Journal of Physiology* **269**, C563–571.

Towbin, H., Staehelin, T. & Gordon, J. (1979). Electrophoretic transfer of proteins from polyacrylamide gels to nitrocellulose sheets: procedure and some applications. *Proceedings of the National Academy of Sciences of the USA* **76**, 4350–4354.

Trinkle-Mulcahy, L., Ichikawa, K., Hartshorne, D. J., Siegman, M. J. & Butler, T. M. (1995). Thiophosphorylation of the 130-kDa subunit is associated with a decreased activity of myosin light chain phosphatase in alpha-toxin-permeabilized smooth muscle. *Journal of Biological Chemistry* **270**, 18191–18194.

Wu, X., Somlyo, A. V. & Somlyo, A. P. (1996). Cyclic GMP-dependent stimulation reverses G-protein-coupled inhibition of smooth muscle myosin light chain phosphate. *Biochemical and Biophysical Research Communications* **220**, 658–663.

Yano, H., Nakanishi, S., Kimura, K., Hanai, N., Saitoh, Y., Fukui, Y., Nonomura, Y. & Matsuda, Y. (1993). Inhibition of histamine secretion by wortmannin through the blockade of phosphatidylinositol 3-kinase in RBL-2H3 cells. *Journal of Biological Chemistry* **268**, 25846–25856.

Acknowledgements

We thank Dr David J. Hartshorne (University of Arizona, Tucson, AZ, USA) for comments and help with the manuscript. This study was supported in part by Grants-in-Aid for Scientific Research (No. 07407022, 10557072), for Scientific Research on Priority Areas (No. 10177222, 10177228), for Encouragement of Young Scientists (No. 10770308), and for Creative Basic Research Studies of Intracellular Signaling Network from the Ministry of Education, Science, Sports and Culture, Japan; and by The Vehicle Racing Commemorative Foundation; Kaibara Morikazu Medical Science Promotion Foundation; Kanae Foundation for Life & Socio-Medical Science; Japan Heart Foundation Research Grant; and Yokoyama Rinshoyakuri and Mochida Memorial Foundation for Medical and Pharmaceutical Research.

Corresponding author

H. Kanaide: Division of Molecular Cardiology, Research Institute of Angiocardiology, Faculty of Medicine, Kyushu University, Maidashi 3-1-1, Higashi-ku, Fukuoka 812-82, Japan.

Email: kanaide@molcar.med.kyushu-u.ac.jp